Conformationally Protected Hydrazine Radical Cations and the Gearing Effect on a Hydrazine Electron-Transfer Reaction

Stephen F. Nelsen,*,† Ling-Jen Chen,† Peter A. Petillo,† Dennis H. Evans,‡ and Franz A. Neugebauer§

Contribution from S. M. McElvain Laboratories of Organic Chemistry, Department of Chemistry, University of Wisconsin, 1101 West University Avenue, Madison, Wisconsin 53706-1396, Department of Chemistry and Biochemistry, University of Delaware, Newark, Delaware 19716, and Abteilung Organische Chemie, Max-Plank-Institut für medizinische Forschung, D-69028 Heidelberg, FRG

Received June 10, 1993®

Abstract: The N-isopropylated hydrazine radical cations from **7** (**22/tBu,iPr**) and **9** (**22/iPr$_2$**) are isolable and are the first examples of isolable hydrazine radical cations which lack all C_α–H bonds being protected as bridgehead carbons in bicyclic rings. The cyclic voltammogram of **9** shows electrochemically irreversible oxidation and reduction waves at platinum. It is argued that this results from a gearing effect of the isopropyl groups, which causes the radical cation from neutral **9** to be generated in an unstable conformation. Kinetic and thermodynamic conformational effects which cause hydrazine cyclic voltammetry curves to be electrochemically irreversible are contrasted.

Isolation of a radical cation, $A^{\cdot+}$, requires not only that this oxidation state be long lived but also that the electron-transfer disproportionation products A^0 and A^{2+} have long enough lifetimes that the proton transfer between them (k_2 in Scheme I) be slow relative to the back-electron-transfer k_{-1}.[1] This is illustrated for a tetraalkylhydrazine radical cation bearing an α-hydrogen in Scheme I. Most hydrazine dications must be extremely potent acids at their α-carbons.

Transfer of an α-proton between A^0 and A^{2+}, shown as eq 2 in Scheme I, is very exothermic. If it were fast enough to compete with back-electron-transfer, $A^{\cdot+}$ would disappear at rates approaching k_1. All published isolated hydrazine radical cations are for cases in which the α-hydrogens are "Bredt's rule kinetically protected", such as **1**. When the C_α–H bonds are at the

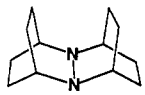

1

bridgeheads of bicyclic systems, the near 90° C_α–H,N^+ (p orbital) twist angle essentially eliminates hyperconjugative bond weakening and the *N*-aminoimmonium cation α-deprotonation product of the dication shown as A^{2+}—H^+ in Scheme I is also destabilized by the bicyclic framework, requiring substantial twist in the C=N bond of the deprotonation product, both factors which will make k_2 much smaller. Apparently as a direct result, bis-bicyclic hydrazine radical cations typically prove isolable.[2] All isolable hydrazine radical cations have shown cyclic voltammograms in acetonitrile which exhibit at least some reversibility for the second oxidation wave. The difference in formal potentials $E°$ for first

Scheme I

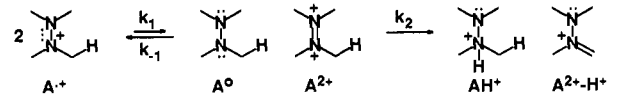

and second electron removal from the bis-bicyclic tetraalkylhydrazines for which both oxidation waves are reversible usually lies in the range 0.9–1.5 V,[2] so k_{-1} must be extremely fast for these systems.[3] The barrier to dication formation by the disproportionation reaction 1 of Scheme I must be at least $23.06\Delta E°$ kcal/mol. It is not clear what $\Delta G°$ is for hydrazines with unconstrained alkyl groups because the second oxidation wave is irreversible. Part of the $\Delta G°$ barrier should be entropic because the components must approach each other in solution to allow electron transfer.[4] Experimentally, when trimethylhydrazines are linked by two to four bridging methylene groups so that they cannot stray far from each other, radical cation lifetimes in a cyclic voltammetry (cv) experiment drop to under a few milliseconds, which we attributed to rapid electron transfer in the bis(radical cation) form to give the neutral, dication form followed by rapid proton-transfer disproportionation.[5]

Sterically imposed conformational constraints on acyclic alkyl groups attached to a charge/spin-bearing center which constrain the p-rich-orbital C_α–H bond twist angles near 90° are also known to greatly increase radical cation lifetimes in solution. A few examples include (hexaethylbenzene)$^{\cdot+}$ [6] and the amine radical

† University of Wisconsin.
‡ University of Delaware.
§ MPI Heidelberg.
® Abstract published in *Advance ACS Abstracts*, October 15, 1993.

(1) We believe the requirement that the electron-transfer disproportionation products as well as the radical cation must be reasonably long lived for isolation of a radical cation was first clearly pointed out by Hünig; see: Hünig, S. *Pure Appl. Chem.* **1967**, *15*, 109.

(2) (a) Nelsen, S. F.; Kessel, C. R.; Brien, D. J. *J. Am. Chem. Soc.* **1980**, *102*, 702. (b) Nelsen, S. F.; Gannett, P. M. *J. Am. Chem. Soc.* **1982**, *104*, 5292. (c) Nelsen, S. F.; Blackstock, S. C.; Frigo, T. B. *J. Am. Chem. Soc.* **1984**, *106*, 3366. (d) Nelsen, S. F.; Blackstock, S. C.; Haller, K. J. *Tetrahedron* **1986**, *42*, 6101. (e) Nelsen, S. F.; Frigo, T. B.; Kim, Y. *J. Am. Chem. Soc.* **1989**, *111*, 5387.

(3) (a) The Eyring free energy barrier for k_{-1} of **1** may be estimated using Marcus cross-rate theory[3b] from $k_{ex}(1^{0/+}$, 298 K, $CH_3CN) = 700\ M^{-1}\ s^{-1}$ ($\Delta G^{\ddagger} = 13.4$ kcal/mol), $k_{ex}(1^{+/2+}$, 298 K, $CH_3CN) = 21\,000\ M^{-1}\ s^{-1}$ ($\Delta G^{\ddagger} = 11.5$ kcal/mol), and $\Delta E° = 1.39$ V,[3c] so $\lambda^{\ddagger}_{-1}/4 = 12.4_7$ and $\Delta G°_{-1} = -32.0_5$ kcal/mol. Since $\Delta G^{\ddagger}_{-1} = (\lambda^{\ddagger}_{-1}/4)(1 - [\Delta G°_{-1}/\lambda^{\ddagger}_{-1}])^2$, $\Delta G^{\ddagger}_{-1} = 1.6$ kcal/mol, indeed a low barrier. (b) For reviews of ET rate theory and those which treat cross-reactions, see: Sutin, N. *Prog. Inorg. Chem.* **1983**, *30*, 441. Eberson, L. *Adv. Phys. Org. Chem.* **1982**, *18*, 79. (c) Nelsen, S. F.; Blackstock, S. C.; Kim, Y. *J. Am. Chem. Soc.* **1987**, *109*, 677.

(4) Using the touching-hard-spheres formula for ΔS (Grampp, G; Jaenicke, W. *Ber. Bunsen-Ges. Phys. Chem.* **1986**, *88*, 335, eq 9) for **1** using the average radius from its crystal structure of 3.95 Å, a ΔS of –6.0 cal deg^{-1} mol^{-1} is obtained, corresponding to a $-T\Delta S$ contribution of 1.8 kcal/mol at room temperature; since this formula does not include solvation effects, which might be substantial, it is not expected to be accurate.

(5) Nelsen, S. F.; Willi, M. R.; Mellor, J. M.; Smith, N. M. *J. Org. Chem.* **1986**, *51*, 2081.

(6) Howell, J. O.; Goncalves, J. M.; Amatore, C.; Klasimo, L.; Wrightman, R. M.; Kochi, J. K. *J. Am. Chem. Soc.* **1984**, *106*, 3968.

0002-7863/93/1515-10611$04.00/0

cations derived from 9-neopentyl-9-azabicyclo[3.3.1]nonane[7] and triisopropylamine.[8] In this work, we report isolation of the first tetraalkylhydrazine radical cations which lack Bredt's rule kinetic protection of all their C_α–H hydrogens and discuss the conformational effects which lead to their isolability on their electron-transfer chemistry.

Results

Compound Preparation, Cyclic Voltammetry, and Radical Cation Characterization. The compounds principally studied here are 2,3-dialkyl-2,3-diazabicyclo[2.2.2]octanes, which we will abbreviate as **22/RR'** where convenient. The parent of this series, **2 (22/Me$_2$)**, is prepared by lithium aluminum hydride reduction of the dicarboethoxy compound[9] and has received considerable study.[10] Because C_α–H deprotonation proceeding as outlined in

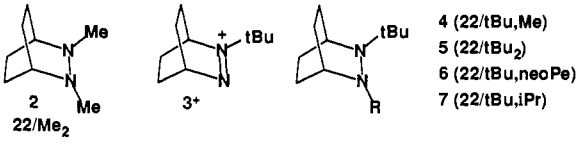

Scheme I was believed to be the reaction leading to decomposition of most hydrazine radical cations, we have investigated *tert*-butylated compounds **4-7**, which were prepared by adding alkyllithiums to the trialkyl diazenium salt **3**$^+$, obtained by *tert*-butylation of 2,3-diazabicyclo[2.2.2]oct-2-ene.[11,12] The diisopropyl compound **9** was prepared by adding isopropylmagnesium chloride to the isopropyl diazenium cation **8**$^+$.[11b,12]

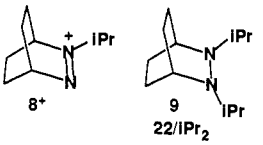

Cyclic voltammetry data for the hydrazines are shown in Table I. Enlarging the size of the alkyl groups makes hydrazine oxidation slightly easier in the absence of steric effects,[10c] but steric effects in both the reduced and oxidized forms clearly are important for these compounds. Replacement of one or both methyl groups of **2** by *tert*-butyl groups affects $E°$ rather little because of the nearly balancing neutral form and radical cation steric destabilization by the *tert*-butyl groups.[13] The isopropyl compound **7 (22/tBu,iPr)** is easier to oxidize than **22/tBu,Me** by 4.8 kcal/mol, which we attribute principally to the larger steric destabilization of the neutral form than of the radical cation. Most tetraalkylhydrazines exhibit electrochemically quasi-reversible cv curves, with a peak-to-peak separation for the oxidation and reduction scans in the range 0.07–0.10 V at 200 mV/s, somewhat larger than the 0.06 V for an electrochemically reversible oxidation. This occurs because of relatively small heterogeneous rate constants k_s for electron transfer, as has been studied in detail for three acyclic hydrazines[14a] and some sesquibicyclic ones.[14b] These small k_s values are probably principally caused by the unusually large Marcus inner sphere reorganization energies for hydrazines.[10c,14] The **22/tBuR** examples substituted with the asymmetrical neopentyl and isopropyl alkyl groups (**6** and **7**) show somewhat larger ΔE_p values than is usual, while the diisopropyl compound **9** has an anomalous cv curve which exhibits electrochemically irreversible oxidation and reduction waves with a 0.37-V peak separation at a 200 mV/s scan rate, which average to about the expected $E°$ value. An increase of about 0.27 V in peak separation relative to **2**, **4**, and **5** corresponds to about 6 kcal/mol, a substantial amount which could in principle be caused by either kinetic or thermodynamic effects. The reason for this increase will be discussed later.

Table I. Cyclic Voltammetry Data[a] for 2,3-Dialkyl-2,3-diazabicyclo[2.2.2]octanes

compound	$E°$, V[b]	ΔE_p, V[c]	k_s, cm/s[d]
2 (22/Me$_2$)[e]	0.07	0.09	0.016
2 (22/tBu,Me)[e]	0.11	0.09	0.016
5 (22/tBu$_2$)[e]	0.03	0.10	0.013
6 (22/tBu,neoPe)	0.13	0.17	0.004
7 (22/tBu,iPr)	–0.10	0.14	0.006
9 (22/iPr$_2$)	–0.04	0.37	0.0007

[a] In acetonitrile containing 0.1 M Bu_4NClO_4, room temperature, 200 mV/s scan rate, potentials reported vs saturated calomel electrode. The results quoted are at a platinum electrode. Significantly more reversible behavior is observed at glassy carbon and gold electrodes, ΔE_p values for **9** of 0.10 and 0.08 V, respectively. Significantly higher k_s values for other hydrazines at gold than at platinum have been previously reported.[14a] [b] Average of oxidation and reduction peak potentials, $(E^{ox}_p + E^{red}_p)/2$. This number is close to $E°$ when electrochemically reversible behavior occurs, which is obviously not the case for **9**. [c] $E^{ox}_p - E^{red}_p$. [d] Standard homogeneous electron-transfer rate constant for direct oxidation to the cation radical, based solely on ΔE_p with $\alpha = 0.70$ (electron-transfer coefficient; defined for the reduction reaction). ΔE_p is only weakly dependent on α for $\Delta E_p < 0.15$ V. [e] From ref 13.

As previously shown,[13] **5 (22/tBu$_2$)**$^{+}$ has a shorter lifetime than most hydrazine radical cations, and its decomposition can be detected at slow scan rates by cv. It decomposes by a different mechanism than most hydrazine radical cations because the cleavage product **3**$^+$ is detected by cv, confirming that *N-tert*-butyl cleavage occurs.[13] Removing C_α–H groups simply by replacing all of them with methyl groups is not the way to obtain an isolable tetraalkylhydrazine radical cation; unlinked vicinal tertiary carbons have too much steric interaction when the nitrogens flatten upon oxidation, making the *N-tert*-butyl bonds too weak for stability at room temperature.

The radical cation from the neopentyl-substituted compound **6** does not decompose as rapidly as **5**$^{+}$, but it is also not isolable. Oxidation with $NOPF_6$ gave a mixture which after recrystallization was mainly an ~88:12 ratio of the aminoimmonium cation **10** and the de-*tert*-butylated diazenium cation **11** (established by ^{1}H NMR), which were not separated. **10** clearly arises from

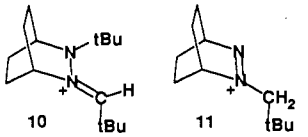

C_α–H deprotonation at the neopentyl group, quite possibly by the electron-transfer/proton-transfer pathway shown in Scheme I. Despite the bulky *tert*-butyl and bicyclic groups sterically shielding the methylene group, it still deprotonates when isolation of **6**$^{+}$ is attempted. The ESR spectrum of **6**$^{+}$ at 178 K shows a major pattern of six very broad lines with an average splitting of 13.8 G and the 1:3:5:5:3:1 intensity distribution expected for

(7) Nelsen, S. F.; Cunkle, G. T. *J. Org. Chem.* **1985**, *50*, 3701.
(8) Bock, H.; Göbl, I.; Havlas, Z.; Liedle, S.; Oberhammer, H. *Angew. Chem., Int. Ed. Engl.* **1991**, *29*, 187.
(9) Anderson, J. E.; Lehn, J. M. *J. Am. Chem. Soc.* **1967**, *89*, 81.
(10) (a) For a review on neutral hydrazine conformations, see: Nelsen, S. F. In *Acyclic Organonitrogen Stereodynamics*; Lambert, J. B., Takeuchi, Y., Eds.; VCH: New York, 1992; Chapter 3, p 89. (b) For a review on nitrogen-centered radical cations, see: Nelsen, S. F. In *Acyclic Organonitrogen Stereodynamics*; Lambert, J. B., Takeuchi, Y., Eds.; VCH: New York, 1992; Chapter 7, p 245. (c) For a review on the electron-transfer reactions of hydrazines, see: Nelsen, S. F. In *Molecular Structures and Energetics*; Liebman, J. F., Greenberg, A., Eds.; VCH Publishers, Inc.: Deerfield Beach, FL, 1986; Vol. 3, Chapter 1, p 1.
(11) (a) Nelsen, S. F.; Landis, R. T., II. *J. Am. Chem. Soc.* **1973**, *95*, 2719. (b) Nelsen, S. F.; Landis, R. T., II. *J. Am. Chem. Soc.* **1974**, *96*, 1788.
(12) Snyder, J. P.; Heyman, M. L.; Gundestrup, M. *J. Chem. Soc., Perkin Trans. 1* **1977**, 1551.
(13) Nelsen, S. F.; Parmelee, W. P. *J. Org. Chem.* **1981**, *46*, 3453.
(14) (a) Kinlen, P. J.; Evans, D. H., Nelsen, S. F. *J. Electroanal. Chem.* **1979**, *97*, 265. (b) Phelps, D. K.; Ramm, M. T.; Wang, Y.; Nelsen, S. F.; Weaver, M. J. *J. Phys. Chem.*, **1993**, *97*, 181.

Table II. a(H) for 2,3-Dialkyl-2,3-diazabicyclo[2.2.2]octane Radical Cations

species	H type	ENDOR (at 210 K)[a]		NMR (at 240 K)[b]		NMR (at 300 K)[b]	
		a(H), MHz	a(H), G	$\delta^{\bullet+}{}_0$[c]	a(H), G[d]	$\delta^{\bullet+}{}_0$[c]	$a(H)_{NMR}$[d]
9$^{\bullet+}NO_3^-$**(22/iPr$_2$)**	H(iPr)	7.31	2.61 (2H)[e]	(unobs)		(unobs)	
	H_x[f]	6.91	2.47 (4H)[e]	(unobs)		(unobs)	
	H_n[f]	−1.63	−0.58	−56.1	−0.61 (4H)[g]	−42.0	−0.59 (4H)[g,h]
	H_{br}[f]	1.02	0.36	47.3	0.48 (2H)[g]	44.4	0.56 (2H)[g,h]
	Me(iPr)	0.50	0.18	16.4	0.17 (12H)[g]	13.2	0.17 (12H)[g,h]
7$^{\bullet+}NO_3^-$**(22/tBu,iPr)**	H_x[f]	7.31	2.61	(unobs)		(unobs)	
	H_x	7.01	2.50	(unobs)		(unobs)	
	i	5.35	1.91	(unobs)		(unobs)	
	i	3.95, 3.36	1.41, 1.20	138.9	1.47	111.6	1.47
	H_n[f]	−1.76	−0.63	−56.8	−0.63 (2H)	−42.9	−0.60 (2H)
	H_n	−1.60	−0.57	−53.0	−0.59 (2H)	−39.3	−0.55 (2H)
	Me(iPr)	0.75	0.27	25.1	0.26 (6H)[g]	19.8	0.25 (6H)[g]
	Me(tBu)	∼|0.25|	∼|0.09|	−6.3	−0.08 (9H)[g]	−4.9	−0.08 (9H)[g]

[a] Solvent: toluene–ethanol containing a trace of CF_3CO_2H. Splittings within ±0.01 G obtained with 95:5 and 80:20 toluene:ethanol mixtures. Signs of splittings established by general triple resonance. [b] Solvent: CD_3CN. [c] Chemical shift for the radical cation hydrogens, extrapolated to zero total radical concentration from a series of spectra run with varying amounts of added di-*tert*-butylnitroxide, in ppm relative to TMS.[17] [d] a(H)[240 K], G = 92.20 ($\delta^{\bullet+}{}_0 - \delta°$), where $\delta°$ is the chemical shift of the same hydrogen in the neutral compound; a(H)[300 K], G = 73.76 ($\delta^{\bullet+}{}_0 - \delta°$).[17] [e] Number of hydrogens responsible for the signal established by special triple resonance. [f] H_x and H_n refer to exo and endo hydrogens at the methylene groups of the bicyclic ring, and H_{br} refers to the bridgehead hydrogens. [g] Relative number of Hs established from the relative size of the NMR peaks. [h] An independent 300 K set of spectra run at $^1/_3$ the concentration gave all five a(H) values within 0.01 G of those reported. [i] The three splittings are assigned to a(CH,iPr) and the two bridgehead splittings. Information is not available to tell which is which; see text.

$a(N) \cong a(N') \cong a(H)$. Rotation about the N–$CH_2$ bond is clearly slow on the ESR time scale, and the N-CH_2 bond angle assumed in the minimum energy conformation causes one CH_2 splitting to be large, about the same size as that for the *N*-methyl compound **4**$^{\bullet+}$, while the other is small and lost in the complex pattern for the bicyclic ring hydrogens. The structure of **6**$^{\bullet+}$ optimized by AM1 semiempirical MO calculations apparently has close to the correct N–CH_2 rotational angle. AM1 predicts the N–CH_2 nitrogen to be planar (average of the three heavy-atom bond angles about nitrogen, α_{av} = 120.00°), the C_αN–CH_2tBu twist angle to be 76.3°, and the NN–CH_2tBu twist angle to be −104.7°, and the C_α–H bonds make twist angles θ of 45.7 and −70.5° ($\cos^2\theta$ = 0.49 and 0.11, respectively) with the p orbital at nitrogen. The splitting constant for these hydrogens should be proportional to $\cos^2\theta$, and $\cos^2\theta$ for a rotating methyl group is 0.5. Thus, AM1 predicts CH_2 hydrogen splitting constants of 0.98 and 0.22 times that of a methyl group at this nitrogen. The methyl hydrogen splitting constant for **4**$^{\bullet+}$ (**22/tBu,Me**) is about 10.5 G,[15] which would lead to predicted splittings of 10.3 and 2.3 G for the methylene hydrogens if the rigid minimum energy conformation was all that gave rise to the spectrum. The actual spectrum is an average over the entire energy surface, the splittings being most sensitive to rotation about the N–CH_2 bond. We have not tried to do this averaging over the AM1 energy surface, but the true minimum energy C_αN–CH_2tBu angle is probably slightly smaller than that calculated by AM1.[16] The ESR spectrum makes it clear that the neopentyl group is not in a conformation which greatly decreases N(π),C_α–H hyperconjugative bond weakening at both CH_2 hydrogens, and experimentally, a C_α–H bond breaks upon attempted isolation of **6**$^{\bullet+}$.

Oxidation of the diisopropyl compound **9** with $AgNO_3$ or $NOPF_6$ gives **9**$^{\bullet+}$ salts as isolable solids. The **9**$^{\bullet+}$ ESR spectrum at 210 K in 8:2 toluene:ethanol shows a(2N) = 13.21 G and a(6H) = 2.56 G, indicating that the *exo* bicyclic ring and the isopropyl group CH splittings are about the same size. The ENDOR spectrum at 210 K (Table II) shows the five different line pairs expected if nitrogen inversion is rapid on the ENDOR time scale and the isopropyl groups are equivalent. Special triple resonance experiments showed that the two-hydrogen isopropyl CH hydrogen splitting is slightly larger than the four-hydrogen *exo* bicyclic ring splitting. Higher temperature NMR experiments using di-*tert*-butylnitroxide as dopant measured the three smaller splittings; the *endo* bicyclic ring splitting is negative and about the same size as those of sesquibicyclic hydrazines,[17] while the bridgehead splitting is positive, is larger than those in sesquibicyclic hydrazines, and appears to be more temperature sensitive than the other small splittings. The isopropyl methyl splitting is very small and positive. Assignments for the smallest splittings could be made from the relative size of the peaks in the NMR spectrum; the very small isopropyl methyl hydrogen splitting is not very distinct in the ENDOR spectrum.

Oxidation of **7** (**22/tBu,iPr**) with $NOPF_6$ or $AgNO_3$ allows isolation of **7**$^{\bullet+}$, which was crystallized to analytical purity. Spectral data for the unsymmetrical **7**$^{\bullet+}$ are complex. The ESR spectrum exhibits a five-major-line pattern showing that the average of the two nitrogen splittings is ca. 13 G. The nine different line pairs expected for rapid nitrogen inversion and one type of (or rapidly equilibrating) isopropyl group(s) were observed by ENDOR at 210 K (Table II). The larger splittings were, as expected, not observed by NMR. The isopropyl CH splitting lies in the range 1.20–1.91 G, so it is significantly smaller than the 2.61 G for those of **9**$^{\bullet+}$. The bridgehead splittings are apparently at least 3.2 times as large as the 0.36-G bridgehead splitting for **9**$^{\bullet+}$ at 210 K, although labeling experiments which would allow for distinguishing the bridgehead splittings from the isopropyl splitting of **7**$^{\bullet+}$ have not been carried out. It is not clear why the 1.20- and 1.41-G splittings observed at 210 K by ENDOR were not resolved in the higher temperature NMR experiments, but the temperature sensitivity of the bridgehead splittings (which were observed to decrease by 0.20 G when the temperature was lowered from 300 to 210 K for **9**$^{\bullet+}$) and the large line width for the signal observed (line width is approximately proportional to the square of ($\delta^{\bullet+}{}_0 - \delta°$) and the signal was too broad to observe except at the higher nitroxide concentrations used) may both contribute to this problem.

Nonbonded steric interactions in the isopropylated hydrazine radical cations **7**$^{\bullet+}$ and **9**$^{\bullet+}$ cause C_α–H,N (lone pair) bond angles which are closer to 90° than that for the larger C_α–H splitting of the neopentyl compound **6**$^{\bullet+}$. The isopropyl CH hydrogen splitting for **9**$^{\bullet+}$ is about 25% as large as that for the unisolable **6**$^{\bullet+}$, and **9**$^{\bullet+}$ can be isolated and stored as the solid. This is

(15) Nelsen, S. F.; Chang, H.; Wolff, J. J.; Adamus, J. Submitted for publication.

(16) Rotation about the N–CH_2 bond to decrease the smaller θ by 5° changes the predicted splittings to 12.1 and 1.3 G, and by 10° to 13.8 and 0.5 G; 5° and 10° increases in the smaller θ change the predictions to 8.4 and 3.6 G and 6.7 and 5.0 G, respectively. Rotation to decrease the smaller θ decreases the C_αN,CH_2tBu angle, so apparently AM1 calculations overestimate this angle by about 5–10°.

(17) For a description of the method and the analysis used, see: (a) Petillo, P. A.; De Felippis, J.; Nelsen, S. F. *J. Org. Chem.* **1991**, *56*, 6496. (b) Nelsen, S. F.; Petillo, P. A.; De Felippis, J.; Wang, Y.; Chen, L.-J.; Yunta, M. J. R.; Neugebauer, F. A. *J. Am. Chem. Soc.* **1993**, *115*, 5608.

consistent with its isolability being a result of smaller C_α–H bond weakening. $7^{\cdot+}$ and $9^{\cdot+}$ may be described as being "conformationally protected" from decomposition, in contrast to previously reported isolable hydrazine radical cations which are Bredt's rule protected.

Neutral and Radical Cation Conformational Effects on cv Curves. The most puzzling aspect of Table I is the electrochemical irreversibility demonstrated by the anomalously large ΔE_p for **9** (**22/iPr$_2$**). Although a significantly smaller k_s value for **9** than those for the other compounds could in principle lead to the large ΔE_p observed, the change in structure between the compounds is so small that we would not expect large differences in k_s. We will argue that the odd behavior of **9** is caused by conformational effects imposed by interaction of the isopropyl groups as electrons are transferred, that is, by a gearing effect. It is necessary to consider the conformations of both the neutral and radical cation forms of **7** and **9** to address this question.

The ^{13}C-NMR spectra of **7** and **9** show that, as expected, both are in *trans* dialkyl conformations which exhibit rapid N–R group rotation but slow double nitrogen inversion on the NMR time scale at room temperature. ^{13}C-DNMR measurements gave estimates for $\Delta G^{\ddagger}$ of double nitrogen inversion (at coalescence temperature T_c): **7**, 18.5 kcal/mol (347 K, DMSO-d_6), **9**, 18.3 kcal/mol (355 K, DMSO-d_6), while line shape analysis gave 17.1 ± 0.3 kcal/mol (350 K, $C_2D_2Cl_4$) for **9**. These enantiomerization barriers are significantly higher than the 12.2 kcal/mol (266 K) of **2** (**22/Me$_2$**) and 13.7 kcal/mol (298 K) of **22/Et$_2$** previously reported,[10a] which is not surprising because the branched alkyl groups must pass each other to achieve the double nitrogen inversion of **7** and **9**. They are not large enough that the enantiomers of **7** or **9** would be separable near room temperature.

The 11 ^{13}C-NMR signals of **7** broaden varying amounts as the temperature is lowered, reaching maximum broadening in the range 180 ± 10 K, and resharpen by 160 K to a single set of 11 signals for the major conformation present. The Me(tBu) signal remains a singlet which appears to broaden near 170 K, but it does not sharpen up as much as the other peaks at 160 K. N-tBu rotation might be just starting to become slow on the NMR time scale. Anet[18] derived simple dynamic NMR equations for this conformational situation of detectable dynamic broadening at intermediate temperature, but the fractional population P of the minor conformation is so small that at low temperature, only peaks for the major conformation can be clearly observed. The peak width at half-height at the temperature of maximum broadening, $\nu(^1/_2\text{max})$ at T_{max}, is related to the frequency difference $\Delta\nu$ between the major and minor conformations by eq 3, while the sum of the rate constants for the conformational

$$\nu(^1/_2\text{max}) = P\delta\nu \qquad (3)$$

change, k(at T_{max}), is given by eq 4. When the free energy

$$k(\text{at } T_{max}) = 2\pi\Delta\nu \qquad (4)$$

difference $\Delta G°$ between the minor and major conformations is large enough to make the minor conformation difficult to see, the barrier corresponding to k(at T_{max}) is dominated by that for change from the minor to major conformation, $\Delta G^{\ddagger}$(min → maj). Although $\Delta G^{\ddagger}$(min → maj) depends upon $\Delta\nu$, the barrier to population of the minor conformation, $\Delta G^{\ddagger}$(maj → min) = $\Delta G^{\ddagger}$(min → maj) + $\Delta G°$, is notably insensitive to $\Delta\nu$ (which is not well known because peaks corresponding to the minor conformation cannot be located). For **7**, 125-MHz spectra recorded at 10° intervals between 240 and 160 K showed large (and, hence, imprecisely measured because of signal to noise problems) $\nu(^1/_2\text{max})$ of ca. 80 Hz for three signals at $T_{max} \simeq$ 190 K (one bridgehead C, one CH_2, and one Me(iPr)), medium $\nu(^1/_2\text{max})$ of 33.2–35.4 Hz for four signals at $T_{max} \simeq$ 180 K (quaternary carbon, CH(iPr), and two CH_2), and small $\nu(^1/_2\text{max})$ of 12.4–13.9 Hz for three signals at $T_{max} \simeq$ 170 K (one bridgehead C, one CH_2, and one Me(iPr)). From eq 3, if P = 0.10, $\Delta\nu$ lies in the range δ 1.0–6.4 for all 10 carbons. Since this is about the range we expect for the $\Delta\nu$ values, it seems unlikely to us that P lies outside the range 0.10 ± 0.05. With this assumption, all 10 peaks fit the ranges $\Delta G^{\ddagger}$(min → maj) 7.3_6 ± 0.12 kcal/mol (if P = 0.05, $\Delta G°$(180 K) = 1.0_5 kcal/mol), $\Delta G^{\ddagger}$(min → maj) 7.6_0 ± 0.13 kcal/mol (if P = 0.10, $\Delta G°$(180 K) = 0.7_9 kcal/mol), $\Delta G^{\ddagger}$(min → maj) 7.7_5 ± 0.14 kcal/mol (if P = 0.15, $\Delta G°$(180 K) = 0.6_2 kcal/mol), and $\Delta G^{\ddagger}$(maj → min) 8.3_9(±0.02) ± 0.14 for P = 0.10 ± 0.05. We believe that this is a plausible isopropyl group rotational barrier for **7**.

Scheme II

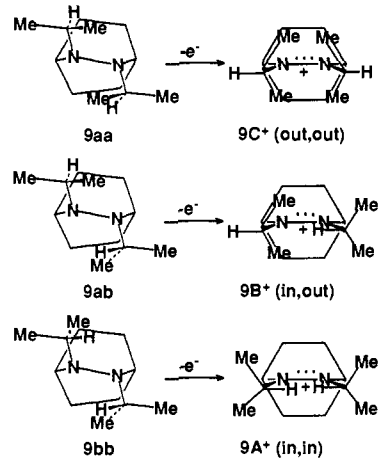

Identification of the major iPr rotamer of **7** is not obvious, and we turned to MM2 calculations[19] using Saunders' stochastic search[20] of the energy surface to locate conformations. The isopropyl group is, as expected, approximately staggered with respect to the nitrogen to which it is attached in all energy minima. It could in principle take up three conformations: with the H–C_α substituent directed toward the bicyclic ring (*anti* to the N lone pair, **7a**), toward the alkyl group on the other nitrogen (*anti* to the N bridgehead bond, **7b**), or *anti* to the NN bond (**7c**). The

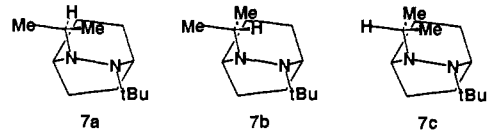

MM2 calculations get the result that **7b** is the conformation with the lowest steric energy, but **7a** is only slightly higher at 0.3 kcal/mol; an extensive Saunders' search which located several different very high energy *syn* conformations did not find an energy minimum corresponding to the obviously strained **7c**. Because MM2 calculations underestimate the energy difference between the two occupied conformations by at least 0.3 kcal/mol and get **7b** and **7a** so close in energy, we do not believe we can reliably predict whether the major observed conformation of **7** is **7b** or **7a** on the basis of these calculations.

It does appear possible to predict reliably that the diisopropyl compound **9** will be significantly more stable in the **9aa** conformation than in any other (see Scheme II). Replacing the tBu of **7** by an isopropyl group in **9** should make the **a** isopropyl rotamer more stable. If a methyl group directed toward the *N'*-tBu group (as it is in **7a**) and toward the bicyclic ring (as it is

(18) (a) Anet, F. A. L.; Yavari, I.; Ferguson, I. J.; Katritsky, A. R.; Morenz-Manas, M.; Robinson, M. T. *J. Chem. Soc., Chem. Commun.* **1976**, 399. (b) Anet, F. A. L.; Basus, V. J. *J. Magn. Reson.* **1978**, *32*, 339.

(19) (a) Allinger, N. L. *J. Am. Chem. Soc.* **1977**, *99*, 8127. (b) Allinger, N. L.; Yuh, Y. *QCPE* **1980**, *12*, 395.

(20) Saunders, M. *J. Am. Chem. Soc.* **1987**, *109*, 3150. We have used VAXMOLE5, most kindly supplied by its author.

Table III. MM2 Calculated Steric Energies for **7** and **9**

conformer	rel E^a	$\angle NNC_iH_\alpha$	tw[b]	$\angle C_iNNC_{i'}$	α_{av}(NiPr)
7 (**22**/tBu, iPr)					
7b	0[c]	−71	10	−122, −124	113.4, tBu 113.7
7a	0.3	69	17	−109, −117	113.8, tBu 111.9
9 (**22**/iPr_2)					
9aa	0[d] (2.1)	65, 65	18	−110, −110	112.3, 112.3
9ab	2.7 (1.1_7)	−69, 62	13	−122, −116	112.1, 113.8
9bb	6.4 (1.2_2)	−69, −69	7	−127, −127	113.5, 113.5
9bc	7.6 (0.4)	−71, 163	8	−125, 124	113.3, 113.3
9cc	10.1 (0.0)	141, 140	5	−124, −124	112.7, 112.7

[a] Difference in MM2 steric energies, in kcal/mol. In parentheses, relative ΔH_f from AM1 calculations (ΔH_f(**9cc**) = 13.68 kcal/mol). [b] Twist in the diazabicyclo[2.2.2]octane system, expressed as $\angle C_bNNC_{b'}$. [c] Steric energy 30.89 kcal/mol. [d] Steric energy 23.53 kcal/mol.

in **7b**) leads to approximately the same steric energy, making the *N'*-alkyl substituent the smaller isopropyl group should significantly stabilize **a** relative to **b**. This is the result MM2 obtains (see Table III), a 3.0 kcal/mol turnaround between **7b** being 0.3 kcal/mol more stable than **7a**, while **9ab** is 2.7 kcal/mol less stable than **9aa**. An extensive Saunders' search located five energy minima up to 11 kcal/mol above **9aa**, including **9bb**, **9bc**, and **9cc**, but did not locate an energy minimum corresponding to the sixth possible *trans* conformation **9ac**. AM1 calculations basically fail for this conformational problem.[21] Low-temperature ^{13}C-NMR studies of **7** showed no line broadening attributable to conformational interconversion down to 200 K, consistent with only **9aa** being sigificantly occupied. Unfortunately, even after comparing the ^{13}C chemical shifts for **9aa** with those for the most stable form of **7**, it is not obvious to us whether this spectrum represents conformation **7a** or **7b**.

Hydrazine radical cations have flattened nitrogens, which will distinctly change the preferred conformation of isopropyl substituents compared to that of the neutral compounds. The small isopropyl C_α–H splittings observed for $7^{\cdot+}$ and $9^{\cdot+}$ show that these CH bonds are nearly perpendicular to the spin-bearing orbital at nitrogen, although the angle cannot be accurately estimated from the splitting constant.[22] The isopropyl C_α–H bonds are then approximately coplanar with the NN bond and can be oriented either "in" or "out" (see Scheme II). We expect the out,in conformation **9B**$^+$ to be less stable than **9A**$^+$ because methyl groups of the out isopropyl are eclipsed with the bicyclic ring methylene groups. **9C**$^+$ should be the least stable because in addition to doubling the amount of 1,3 alkyl,alkyl eclipsing, it will have nonbonded methyl,methyl steric interactions between the isopropyl groups. AM1 calculations get **9A**$^+$–**9C**$^+$ in this energy order but obtain **9A**$^+$ and **9B**$^+$ at nearly the same energy,[23] which is experimentally incorrect. The ENDOR experiments indicate that only a symmetrical conformation is present at the detectable concentration at 210 K, which can be reliably assigned as **9A**$^+$. We expect isopropyl group rotation in $9^{\cdot+}$ to be frozen out on the ENDOR time scale at 210 K, so that if an unsymmetrical and symmetrical conformation had nearly the same energy, two sets of signals would be observed. If the unsymmetrical conformation **9B**$^+$ were significantly destabilized relative to **9A**$^+$, it would be present in such a small concentration relative to that of **9A**$^+$ that it would not be observed; a 1.1 kcal/mol free energy difference would give 6% of the minor isomer at 210 K. Once again, AM1 has underestimated the energy difference between different conformations. We presume that $7^{\cdot+}$ is in the hydrogen in conformation **7A**$^+$ because the large *tert*-butyl group should significantly destabilize the hydrogen out conformation.

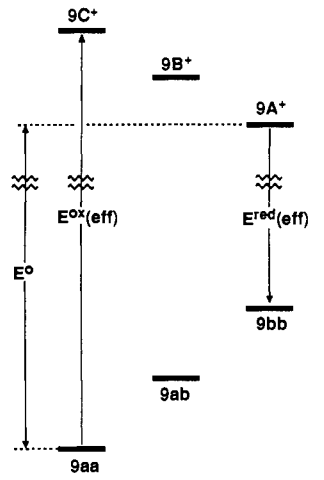

Figure 1. Energy diagram indicating the effective oxidation and reduction potentials for **9** in a cv experiment, assuming that **9aa** oxidizes to **9C**$^+$ and **9A**$^+$ reduces to **9bb** (see Scheme II).

Discussion

cv Curves for 9 (22/iPr_2). We suggest that the key to understanding the large peak separation in the cv of **9** is the consideration of what conformations the change in interactions between the alkyl groups as electron transfer occurs will produce (see Scheme II). Removal of an electron from **9aa** will flatten the nitrogens, increasing steric interaction between the methyl groups pointing "in" in the neutral form which will cause the isopropyl groups to both undergo counterclockwise rotation in the view shown, which will produce **9C**$^+$, the least stable isopropyl rotamer of $9^{\cdot+}$. The only conformation of **9** shown which would directly produce the most stable conformation of the cation **9A**$^+$ is **9bb**, which has both isopropyl C_α–H bonds directed inward and is substantially destabilized relative to **9aa**. The oxidation products shown in Scheme II are the conformations produced by AM1 calculations of the radical cation starting from the geometry of the neutral compound. Isopropyl group rotation in $9^{\cdot+}$ should be rather rapid because the nitrogen is nearly planar, producing an sp^2,sp^3 6-fold barrier. Conversion of **9C**$^+$ produced by electron loss from **9aa** to the more stable rotamer **9A**$^+$ should be rapid on the time scale of the scan rates available in our cv experiments so that no reduction wave for **9C**$^+$ to **9aa** would be seen. Instead, the potential would need to reach a value where **9A**$^+$ that was produced during the oxidation wave could be reduced to **9**. If **9A**$^+$ reduced to the significantly destabilized **9bb**, the effective formal potential for reduction (the **9A**$^+$,**9bb** free energy gap) would be significantly more negative than the effective formal potential for oxidation (the **9aa**,**9C**$^+$ energy gap). A schematic diagram for the situation described is shown as Figure 1 and the electrochemical scheme which results as Figure 2 ($E^o_{i,j}$ denotes the reversible formal potential for the i + e^- ⇌ j couple). The gearing effect indicated in Figures 1 and 2 is proposed to account

(21) We have recently compared the ability of MM2 and semiempirical AM1 calculations to reproduce the X-ray geometries of hydrazines; see: Nelsen, S. F.; Wang, Y; Powell, D. R.; Hiyashi, R. K. *J. Am. Chem. Soc.* **1993**, *115*, 5246. The conclusion was that MM2 calculations might be expected to do a fairly reasonable job on relative energies of conformations of these hydrazines but AM1 calculations will not be able to do so. AM1 heats of formation are in essentially the reverse order of relative energy as those of MM2: **9aa**, 2.1; **9ab**, 1.1_7; **9bb**, 1.2_2; **9bc**, 0.4; **1cc**, 0.0 kcal/mol. We believe it is certain that the AM1 ordering is incorrect, and note that the range of isopropyl rotamer energy differences is considerably underestimated by AM1.

(22) The usual formula $a(H) = B\cos^2\theta\,\lambda_\pi$ is not accurate for this kind of system when θ is near 90°, apparently because of the large spin density of opposite sign at the adjacent nitrogen.[17]

(23) (a) AM1-UHF calculations get relative energies of: **9A**$^+$, 0.0; **9B**$^+$, 0.07; **9C**$^+$, 4.18 kcal/mol. (b) For 2,3-diisopropylbicyclo[2.2.2]oct-2-ene, where both MM2 and AM1 get comformations with essentially no bicyclic ring torsion, the relative energies of isopropyl group rotomers are similar: MM2 A (**in,in**) 0.0 (SE 25.66 kcal/mol), B (**in,out**) 1.7, C (**out,out**) 8.0; AM1 A 0.0 (ΔH_f −36.88 kcal/mol), B 1.1, C 5.6. This suggests that the energy difference between **9A**$^+$ and **9C**$^+$ is more likely to be underestimated than overestimated by AM1.

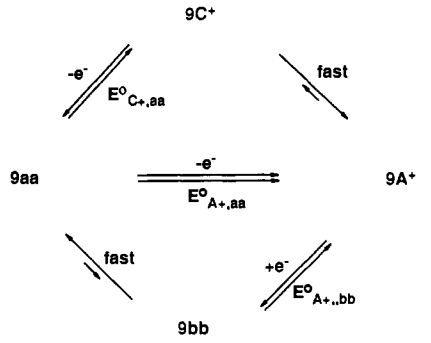

Figure 2. Redox scheme for **9** assuming the conformational consequences of SchemeII and Figure 1.

for the large increase in cv peak separation observed for **9** compared to those for most other hydrazines. For a complete description of "gear-meshed" isopropyl groups in hexaisopropylbenzene, see Mislow et. al.[24]

The scheme shown in Figure 2 is known in electrochemistry as a square scheme[25] in which, in this case, the left and right hand corners of the square are occupied by the most stable forms for the neutral hydrazine and the radical cation, respectively. The upper and lower corners represent destabilized forms of the two oxidation states. The form of the voltammetric response that one obtains depends in a complex manner on the relative values of $E^{\circ}_{C+,aa}$, $E^{\circ}_{A+,bb}$, and the equilibrium constants $K_{C^+,A^+} = k_{C^+\rightarrow A^+}/k_{A^+\rightarrow C^+}$ and $K_{aa,bb} = k_{aa\rightarrow bb}/k_{bb\rightarrow aa}$ as well as the magnitude of the rate constants for heterogeneous electron transfer and conformational changes.[26 a]

Using a simulation program based on the heterogeneous equivalent method,[26] it was possible to reproduce the main features of the cyclic voltammograms of **9** under square-scheme conditions in which oxidation occurs by the EC (an electrode reaction followed by a reversible chemical reaction) upper path of Figure 2, **9aa** → **9C**$^+$ → **9A**$^+$, and reduction follows the EC lower path sequence **9A**$^+$ → **9bb** → **9aa**, viz., $K_{C^+,A^+} = 2.5 \times 10^4$ (ΔG°(**C**$^+$,**A**$^+$) = –6 kcal/mol) and $K_{aa,bb} = 1.9 \times 10^{-5}$ (ΔG°(**aa**,**bb**) = 6.4 kcal/mol); rate constants in the faster direction are set at 10^7 s^{-1}. In particular, the change in peak separation for a 50-fold change in scan rate (0.02–1.0 V/s) was accurately reproduced, and the relative peak heights (anodic vs cathodic) were also reasonably correct. However, the detailed shapes of the current-potential curves, particularly in the rising portion of each peak, were not well reproduced. Much better fits to the experimental cv curves were obtained when it was assumed that the system falls into another kinetic regime, viz., the situation where the rate constants for the **9C**$^+$,**9A**$^+$ conversion are large enough that the back reaction **9A**$^+$ → **9C**$^+$ is significant on the voltammetric time scale so that most of the reduction proceeds by the CE sequence **9A**$^+$ → **9C**$^+$ → **9aa**. An example of a fit of simulation to an experimental voltammogram is shown in Figure 3, and the results for five other scan rates between 0.02 and 1.0 V/s are given in the supplementary material. The common set of parameters used in all six simulations is given in Table IV, set 1. A perusal of these parameters will be informative. First, even at a 1 V/s scan rate, the largest used, over 80% of the reduction follows the upper CE path of Figure 2, **9A**$^+$ → **9C**$^+$ → **9aa**. For this reason, the simulations are only weakly dependent on the parameters of the lower half of the square scheme (Figure 2; Table IV, footnote *c*). As is well known for an EC scheme,[27] the parameters K_{C^+,A^+} and $k_{C^+\rightarrow A^+}$ are coupled, only $K_{C^+,A^+}/(k_{C^+\rightarrow A^+})^{1/2}$ being extractable from the voltammogram. A variety of values for these two parameters in addition to those listed as set 1 in Table IV is possible, but they are limited by the reasonable range of free energies of activation one would expect for the isopropyl group rotation in **9**$^{\cdot+}$ and the fact that **9C**$^+$ is sterically destabilized relative to **9A**$^+$, so K_{C^+,A^+} must be large. For example, by using the parameters of set 2, Table IV, simulations which match the experiments as well as the first entries are produced. The values of $E^{\circ}_{C^+,aa}$ and k_s(**C**$^+$,**aa**) are also intertwined with the two parameters mentioned above, as shown in Table IV. The two were chosen to approximate the range of k_s values for "normal" hydrazines (see Table I) where ΔE_p is 0.09–0.14 V at 0.2 V/s scan rates. However, ΔE_p is 0.37 V for **9** with the same range of heterogeneous rate constants k_s. This is an example of a fast chemical reaction (the **9C**$^+$,**9A**$^+$ conformational change) affecting electron-transfer kinetics. When the conversion of **9C**$^+$ to **9A**$^+$ becomes fast enough, it competes with the back-electron-transfer reaction forcing the forward electron-transfer reaction (**9aa** → **9C**$^+$ + e$^-$) to become rate-limiting.[28,29] Thus, the process is observed to be totally electrochemically irreversible with a very large separation in peak potentials rather

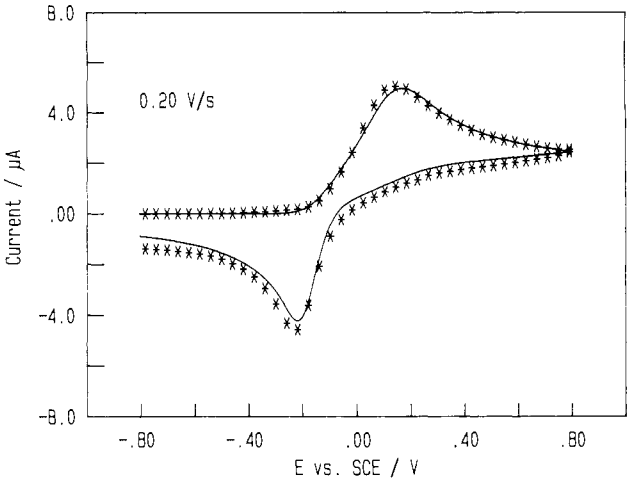

Figure 3. Cyclic voltammogram of 0.5 mM **9** at 0.20 V/s and room temperature: curve, simulation using parameters listed in Table IV, set 1, and points, experimental.

Table IV. Parameters for Simulation of the Voltammogram in Figure 3[a]

	set 1	set 2
$E^{\circ}_{C^+,aa}$, V vs SCE[b]	0.08	0.14
$E^{\circ}_{A^+,aa}$, V vs SCE[b]	–0.12	–0.12
K_{C^+,A^+} (ΔG°(**C**$^+$,**A**$^+$), kcal/mol)[b]	2.50×10^3 (–4.6)	2.50×10^4 (–6.0)
$k_{C^+\rightarrow A^+}$, s^{-1} ($\Delta G^{\ddagger}$, kcal/mol)[b]	3.89×10^8 (5.7)	3.89×10^{10} (3.0)
$k_{A^+\rightarrow C^+}$, s^{-1} ($\Delta G^{\ddagger}$, kcal/mol)[b]	1.56×10^5 (10.4)	1.56×10^6 (9.0)
k_s(**C**$^+$,**aa**), cm/s[b]	7.42×10^{-3}	2.5×10^{-2}
α(**C**$^+$,**aa**)	0.70	
$E^{\circ}_{A^+,bb}$, V vs SCE[c]	–0.40	
$K_{aa,bb}$, (ΔG°(**aa** → **bb**), kcal/mol)[c]	1.92×10^{-5} (6.4)	
$k_{bb\rightarrow aa}$, s^{-1} ($\Delta G^{\ddagger}$, kcal/mol)[c]	3.89×10^7 (7.1)	
$k_{aa\rightarrow bb}$, s^{-1} ($\Delta G^{\ddagger}$, kcal/mol)[c]	7.47×10^2 (13.5)	
k_s(**A**$^+$,**bb**), cm/s[c]	4.95×10^{-2}	
α(**A**$^+$,**bb**)[c]	0.40	

[a] All calculations at 298 K. Electron-transfer coefficients (α) defined for reduction, i.e., $k_{red} = k_s \exp[((1-\alpha)F/RT)(E-E^{\circ})]$. To evaluate k_s, the diffusion coefficient was assumed to be 2×10^{-5} cm^2/s. Geometrical parameter accounting for edge diffusion: $D^{1/2}/r = 0.1$ s$^{-1/2}$. [b] Coupled parameters. [c] Simulations relatively insensitive to this parameter.

(24) Siegel, J.; Gutiérrez, A.; Schweizer, W. B.; Ermer, O.; Mislow, K. *J. Am. Chem. Soc.* **1986**, *108*, 1569.
(25) Evans, D. H. *Chem. Rev.* **1990**, *90*, 739.
(26) (a) Lerke, S. A.; Evans, D. H.; Feldberg, S. W. *J. Electroanal. Chem.* **1990**, *296*, 299. (b) Ruzic, I.; Feldberg, S. W. *Ibid.* **1974**, *50*, 153. (c) The program included hemispherical diffusion with the geometrical parameter $(D/a)^{1/2}/r$, where $a = Fv/RT$, v is the scan rate, and r is the radius of the electrode. This procedure accurately mimics the effects of diffusion from the periphery of the disk electrode so long as the effects are small, as is true in the present case. The geometric parameter was treated as adjustable, and the best fit value for $D^{1/2}/r$ was about twice the actual value calculated using the disk radius.
(27) Nicholson, R. S.; Shain, I. *Anal. Chem.* **1972**, *36*, 706.
(28) Evans, D. H. *J. Phys. Chem.* **1972**, *76*, 1160.
(29) Nadjo, L.; Savéant, J. M. *J. Electroanal. Chem.* **1973**, *48*, 113.

than exhibiting the smaller ΔE_p characteristic of the relatively large k_s for the electron transfer.

The ET process can also be modeled as a direct, electrochemically irreversible oxidation following the horizontal reaction of Figure 2, **9aa** $\rightleftharpoons$ **9A**$^+$ + e$^-$. Simulations (not shown) produce good fits to the data with $E°_{A^+,aa} = -0.11$ V vs SCE, $\alpha = 0.70$, and $k_s(A^+,aa) = 7.4 \times 10^{-4}$ cm/s. It is noteworthy that this k_s value is about an order of magnitude lower than those of the structurally similar hydrazines **2-7**. According to this interpretation, the lower value of k_s for **9** compared to those for **2-7** would be due to an inner-sphere reorganization energy for **9** that is larger than those for the other hydrazines. It would have to be postulated that ΔG^*_{in} is 1.6 kcal/mol, or λ_{in} is 6.4 kcal/mol, larger for **9** than for the average of **2-7** for the direct oxidation to be the mechanism.

To summarize, the voltammetric data can be equally well accounted for by either of two mechanisms: the CE/EC scheme (upper pathway of the square scheme of Figure 2) or the direct electron-transfer scheme (horizontal path through Figure 2). We favor the first of these interpretations because it is consonant with the existence of intermediate **9C**$^+$, which is expected to be generated smoothly from **9aa** upon electron loss by a gearing effect. Also, reasonable values for the free energy gap between **9C**$^+$ and **9A**$^+$ and the rate constant for this conformational change were found to account for the data. Finally, analysis according to the square scheme produces the satisfying result that k_s(**C**$^+$,**aa**) is in the same range as the values for hydrazines of very similar structure, thus avoiding the necessity of invoking some special effect to account for the smaller k_s would have **9** to exhibit for the direct oxidation scheme to be involved.

Comparison with Hexahydropyridazine cv Studies. Low-temperature cv work on chair hexahydropyridazine derivatives has demonstrated large conformational effects,[30] but we believe they are significantly different ones from those postulated above for **9**. We shall abbreviate hexahydropyridazine as **P** followed by **a**, axial, and **e**, equatorial, for identification of the *N*-alkyl substituent stereochemistry. When conformational interconversion is slow on the cv time scale, separate oxidation waves are observed for the lone pair,lone pair twist angle $\theta \simeq 180°$ diequatorial alkyl-substituted **Pee** conformations and the $\theta \simeq 60°$ **Pae** conformations. The waves for **Pee** are electrochemically quasi-reversible and appear near the potentials of the high-temperature-limit voltammogram, but the **Pae** oxidation wave is irreversible and appears at a considerably higher potential than that for **Pee**. The single reduction wave observed corresponds in current to reduction of the radical cation formed from both the **Pee** and **Pae** conformations. It was pointed out that this behavior would occur if either of two oxidation pathways were followed (see Figure 4). (1) **Pee** and **Pae** conformations oxidize to different radical cations (**Pee**$^{\cdot+}$ and **Pae**$^{\cdot+}$ of Figure 4), with $E°$(**ae**) significantly higher in potential than $E°$(**ee**), but the conformational change from **Pae**$^{\cdot+}$ to **Pee**$^{\cdot+}$is so rapid that no reduction of **Pae**$^{\cdot+}$ is observed at the fastest scan rates, (i.e., the pathway following the outer square of Figure 4). (2) **Pee** and **Pae** oxidize to the same, relaxed radical cation (**Pee**$^{\cdot+}$ of Figure 4), but the heterogeneous electron-transfer rate constant k_s(**ae**) is very small (i.e., the triangular pathway following the diagonal, irreversible oxidation pathway of Figure 4). These schemes are kinetically equivalent in the absence of observing the reduction of **Pae**$^{\cdot+}$, and the observed cv curves were successfully analyzed using the triangular scheme. In studies of *N,N'*-disubstituted dihydrobenzocinnolines which exist exclusively in **aa** conformations, Heinze, Neugebauer, and co-workers[31] stated that they obtained evidence for the square scheme for these compounds whose electrochemistry is complicated by showing oxidation only to the dication. In order for the square scheme to be involved, it appears that **Pae**$^{\cdot+}$ must be an energy minimum conformation. This seems highly unlikely for hexahydropyridazine derivatives. Twisting at the NN bond of hydrazine radical cations is costly in energy,[32] and not surprisingly, we have been unable to find a significantly twisted energy minimum using AM1 calculations; we can see no structural reason for the alkyl groups to lock **P**$^{\cdot+}$ into a twisted conformation. It also appears that flattening the nitrogens of neutral hexahydropyridazine conformations does not lead to high energy forms of the radical cation (i.e., the situation discussed above for **9** appears not to occur). AM1 calculations of the parent dimethylhexahydropyridazine radical cations **12**$^{\cdot+}$ starting from the geometries of neutral **12ee** and **12ae** give the same (very slightly) *anti* bent structure, $\Delta H_f = 184.49$ kcal/mol, while starting from **12aa** gives the (very slightly) *syn* bent structure, $\Delta H_f = 184.32$ kcal/mol. The energy difference is a trivial 0.17 kcal/mol, and both have untwisted half-chair structures which have been shown by ESR work to be those of the relaxed radical cations.[33] If an energy minimum twisted **Pae**$^{\cdot+}$ conformation is not present, it does not appear that writing such a species as an intermediate is reasonable, and the square scheme for **P** redox reactions shown in Figure 4 would not be plausible.

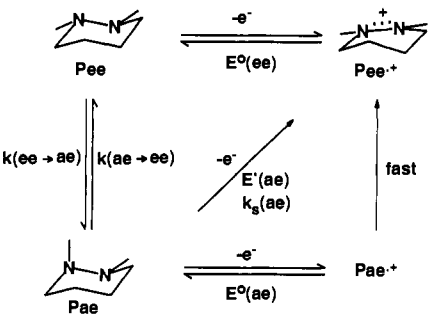

Figure 4. Square and triangular redox schemes for a hexahydropyridazine derivative, **P** (illustrated with *N*-alkyl groups as the only substituents). Axial and equatorial *N*-alkyl groups are designated **a** and **e**, respectively.

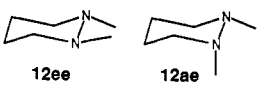

Hydrazine Relaxation Energies and k_s Values. Something that bothered us for years was the necessity of postulating slow heterogeneous ET for **Pae**, $\theta \simeq 60°$, but much faster heterogeneous ET for **2** (**22/Me$_2$**), $\theta \simeq 120°$, because small ΔE_p values, comparable to conformationally unrestricted hydrazines, are observed by cv (Table I). This appeared anomalous because the vertical radical cations are both twisted about 60° from the coplanar $\theta \simeq 0°/180°$ value of their relaxed radical cations.

More is known now about hydrazine relaxation energies than when the low-temperature cv work was carried out in the late 1970s. If we use the letters n and c to represent the relaxed geometry of the neutral and the radical cation and the superscripts o and + for the charge present, the enthalpy portion of the Marcus λ_{in} value, which we will call λ'_{in}, for a self-ET is the enthalpy difference between the vertical electron-transfer pair and the

(30) (a) Nelsen, S. F.; Echegoyen, L.; Evans, D. H. *J. Am. Chem. Soc.* **1975**, *97*, 3530. (b) Nelsen, S. F.; Echegoyen, L.; Clennan, E. L.; Evans, D. H.; Corrigan, D. A. *J. Am. Chem. Soc.* **1977**, *99*, 1130. (c) Evans, D. H.; Nelsen, S. F. In *Characterization of Solutes in Non-Aqueous Solvents*; Mamantov, G., Ed.; Plenum Press: New York, 1978; p 131. (d) Nelsen, S. F.; Clennan, E. L.; Evans, D. H. *J. Am. Chem. Soc.* **1978**, *100*, 4012.

(31) Dietrich, M.; Heinze, J.; Fischer, H.; Neugebauer, F. A. *Angew. Chem., Int. Ed. Engl.* **1986**, *105*, 1021.

(32) Nelsen, S. F.; Cunkle, G. T.; Evans, D. H.; Haller, K. J.; Kaftory, M.; Kirste, B.; Clark, T. *J. Am. Chem. Soc.* **1985**, *107*, 3829.

(33) Nelsen, S. F.; Yumibe, Y. *J. Org. Chem.* **1985**, *50*, 4749.

starting pair (eq 5):[34] This may be rewritten as the sum of the

$$\lambda'_{in} = [\Delta H_f(n^+) + \Delta H_f(c^\circ)] - [\Delta H_f(n^\circ) + \Delta H_f(c^+)] \quad (5)$$

relaxation energies of the cations and the neutral species (eq 6).

$$\lambda'_{in} = [\Delta H_f(n^+) - \Delta H_f(c^+)] + [\Delta H_f(c^\circ) - \Delta H_f(n^\circ)] = \Delta H_r(cat) - \Delta H_r(neu) \quad (6)$$

Using these equations allows consideration of the effect of twisting about the NN bond on λ'_{in}. Fortunate (and unanticipated) cancellation of errors in calculating ΔH_r(cat) occur for AM1 calculations on hydrazines,[35] making their results far superior to 6-31G* *ab initio* calculations. Figure 5 shows a plot of calculated λ'_{in} for tetramethylhydrazine as a function of NN rotational angle θ. It may be noted that the maximum is displaced toward a smaller θ than 90° and that the calculations predict significantly higher λ'_{in} values in the θ range 50°–80° (54–61 kcal/mol) than in the range 110°–140° (46–40 kcal/mol). Obviously, there is no guarantee that these calculations give a correct picture of how even the AM1-calculated λ'_{in} will change with θ because other geometry changes at the nitrogen will occur when alkyl substituents force θ to be far from the electronically preferred near-90° value. As shown below, rather similar values are in fact calculated for examples of compounds with rings which cause such θ values; Figure 5 does appear to be useful in considering λ'_{in} for hydrazines.

There is no experimental way of determining ΔH_r(neu), but ΔH_r(cat) is accessible; it is the difference between the vertical and adiabatic ionization potentials (vIP and aIP, respectively):

$$\Delta H_r(cat) = vIP - aIP \quad (7)$$

Gas-phase measurements have given experimental values of vIP – aIP for several hydrazines,[36] and AM1 calculations of ΔH_r(cat) do a surprisingly good job of calculating these numbers.[34,37] It may be noted from Figure 5 that only ΔH_r(cat) changes very significantly with θ. For a comparison of the compounds of interest here, see Table V which includes compounds **13-15**. In particular,

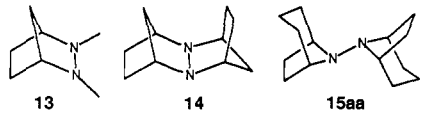

13 14 15aa

the far higher ΔH_r(cat) values for *gauche* hydrazines like tetramethylhydrazine and **12ae** than those for *anti* hydrazines like **2 (22/Me$_2$)** are calculated to occur (several similar examples were also studied[36]), and numbers of approximately the right size are obtained by AM1 calculations. This encourages us to assert that the AM1-calculated λ'_{in} values, also shown in Table V, are likely to be reasonably useful.

We suggest that the calculations summarized in Table V allow five points to be made.

(1) The electrochemical irreversibility observed experimentally for the **Pae** form by cyclic voltammetry is consistent with the triangular scheme because the large difference in the k_s values required is expected from the difference in the λ'_{in} values required from the vIP and aIP measurements. An electron-exchange rate constant should be given by k_{ex} = PRE exp(-$\Delta G^*/RT$). For systems as similar as **Pee** and **Pae**, we believe it should be an excellent approximation that the preexponential factor PRE and

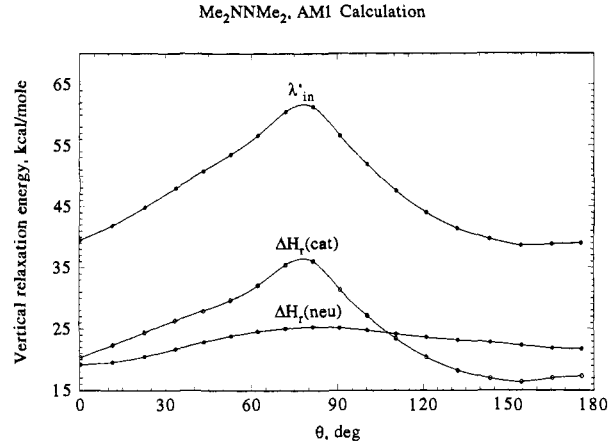

Figure 5. AM1 calculations of λ'_{in} for tetramethylhydrazine as a function of the NN rotational angle θ.

Table V. Experimental and Calculated Relaxation Energies for Hydrazines

compound	vIP – aIP (exper[7])	ΔH_r(cat) (AM1)	ΔH_r(neu) (AM1)	λ'_{in} (AM1)	θ (AM1)	θ (MM2)
Me$_2$NNMe$_2$	32.1	33.2	25.3	58.5	83.4	89.3
12ae	30.7	30.2	24.5	54.7	56.5	69.1
12ee	22.1	17.6	22.6	40.2	176.7	178.2
2(22/Me$_2$)	23.3	20.1	24.6	44.6	129.0	117.8
4(22/tBu,Me)		19.3	27.2	46.5	126.7	119.8
13(21/Me$_2$)	23.1	19.4	24.7	44.1	128.2	124.5
14(21/21)	18.9	15.8	19.5	35.7	0.0	0.0
15[a]		15.1	19.7	34.9	180.0	180.0

[a] For the *anti* **aa** form illustrated. This is 2.2 kcal/mol lower than that of the θ = 81.4° *gauche* form by AM1, but neither MM2 calculations nor experiments (see text) get *gauche* forms as significant for **15**.

the outer-sphere contributions to ΔG^* ought to be the same. Therefore, we expect that the ratio of k_s values for heterogeneous ET for the **ae** and **ee** forms of **P** should be k_s(**ae**)/k_s(**ee**) = exp(-$\Delta\lambda'_{in}/8RT$). Using the AM1-calculated λ'_{in} values, this produces k_s(**ae**)/k_s(**ee**) = 1.53 × 10^{-2} at 218 K. The k_s(**ae**)/k_s(**ee**) ratio adjusted for best fit to the experimental data for 1,2,3-trimethylhexahydropyridazine at 218 K in our low-temperature cv work using the triangular reaction scheme was 3.29 × 10^{-3}.[37]

(2) Despite the large difference in θ for **Pee** (~180°) and **2 (22/Me$_2$)** (~120°), k_s is predicted to be similar for these two compounds both from the similar ΔH_r(cat) values measured by high-pressure mass spectrommetry[36] and from the AM1 calculations, as required by their experimental cyclic voltammograms. The difference in experimental values of vIP – aIP is 1.2 kcal/mol, and in calculated λ'_{in} is 4.44 kcal/mol. Using the larger λ'_{in} difference (and one could argue that the smaller experimental vIP – aIP difference would be the one we should use), we obtain k_s(**2**)/k_s(**12**) = 0.15, which is consistent with the small difference in ΔE_p observed in cv curves.

(3) According to AM1, only *gauche* hydrazines are predicted to have significantly higher λ'_{in} than are 180° hydrazines. This is consistent with our not being able to find temperature-dependent cv curves for *N,N'*-bicyclic hydrazines similar to those for hexahydropyridazines.

(4) **14 (21/21)** is calculated to have significantly lower λ_{in} than are the compounds above it in Table V. This is consistent with the faster homogeneous self-ET observed for sesquibicyclic compounds such as **14**.[38] Of the compounds in Table V, only **14** has fast enough self-ET to observe NMR line broadening.

(5) AM1 calculations of ΔH_r(cat), and hence of λ'_{in}, do not work well for all tetraalkylhydrazines. If the calculations seriously

(34) (a) Nelsen, S. F.; Blackstock, S. C; Kim, Y. *J. Am. Chem. Soc.* **1987**, *109*, 677. (b) Nelsen, S. F. Internal Geometry Relaxation Effects on Electron Tranfer Rates of Amino Centered System. In *Advances in Electron Transfer Chemistry;* Mariano, P. S., Ed.; JAI: Greeenwich, CT; Vol. 3.

(35) Unpublished calculations by P. A. Petillo and S. F. Nelsen.

(36) Nelsen, S. F.; Rumack, D. T.; Meot-Ner (Mautner), M. *J. Am. Chem. Soc.* **1988**, *110*, 7945.

(37) See ref 30b. The ΔE° used in these simulations was 3 kcal/mol instead of the much smaller number obtained from the ratio of about 10% ee present at 218 K, and as is pointed out, α-values also affect the fit.

(38) (a) Nelsen, S. F.; Blackstock, S. C. *J. Am. Chem. Soc.* **1985**, *107*, 7189. (b) Nelsen, S. F.; Kim, Y.; Blackstock, S. C. *J. Am. Chem. Soc.* **1989**, *111*, 2045.

enough err in estimating the geometry, they presumably will also err in calculating λ'_{in}. The relative success of AM1 in calculating the geometries of tetraalkylhydrazines with various substitution patterns has been recently discussed.[21] The relative energies of **12** conformations are not handled properly by AM1 calculations, which get the stability order backwards. ΔH_r(cat) for the *anti* form **12ee** is calculated to be 4.5 kcal/mol larger than the experimental value, but ΔH_r(cat) is well estimated by AM1 for the *gauche* form **12ae** (Table IV). A good example of a system where errors in estimated λ'_{in} values are large occurs for **15**. A low λ'_{in} value is calculated for the *anti* isomer shown as **15aa**, which is the most stable *anti* isomer by AM1. *Anti* forms of **15** are known to be present in the gas phase (PE measurement) and in the crystal (X-ray crystallography) and also appear to be those present in solution from ^{13}C-NMR measurements. However, **15** experimentally exhibits slow self-ET,[32] which is incompatible with the calculated λ'_{in} value. However, AM1 makes serious errors in estimating the geometry of neutral **15**. It calculates the **15aa** *anti* form shown to be the more stable one, while NMR measurements show that it is the less stable *anti* form in solution. More seriously, AM1 calculates the *gauche* form to be 2.2 kcal/mol more stable than any *anti* form, which is incorrect. AM1 does produce a larger calculated λ'_{in} for the *gauche* form but still predicts rapid self-ET through the *anti* form for **15**. Either the λ'_{in} calculated by AM1 for **15** must be counted as a significant failure for AM1 to estimate a reasonable λ'_{in} value or the preexponential term for **15** self-ET must be significantly lower than those for sesquibicyclic hydrazines, which we consider unlikely. The surprising thing about the AM1 calculations of λ'_{in} is that they work as well as they do, not that they fail badly for some cases. AM1 calculations appear to produce λ'_{in} values usefully close to the true values for *N,N'*-bicyclic hydrazines, the class of compounds discussed here.

Conclusion

Isopropyl groups as nitrogen substituents on the diazabicyclooctane system provide enough kinetic protection from deprotonation by steric interactions which force their C_α–H bonds into low bond-weakening conformations to allow $\mathbf{7}^{\cdot+}$ and $\mathbf{9}^{\cdot+}$ to be isolated. $\mathbf{6}^{\cdot+}$ **(22/neoPe)** undergoes proton-transfer decomposition upon attempted isolation despite substantial steric protection of its α-methylene group, presumably because one C_α–H bond is in a conformation which weakens it. The electrochemically irreversible cv behavior of **9 (22/iPr$_2$)** at a platinum electrode is consistent with the square scheme of Figure 2; gearing of the isopropyl groups makes the oxidation of **9** produce a destabilized form of $\mathbf{9}^{\cdot+}$. Calculations show that the destabilized energy minima required for the above rationalization to be true are indeed present on the energy surface for $\mathbf{9,9}^{\cdot+}$, although the calculations are not accurate enough to provide accurate relative energies of these conformations. The triangular scheme of Figure 4 for hexahydropyridazine oxidation is consistent with the small k_s values predicted for **Pae** oxidation, and the $\mathbf{P,P}^{\cdot+}$ energy surface is calculated not to have the energy minimum present for $\mathbf{Pae}^{\cdot+}$ which is necessary for the square scheme shown in Figure 4. We therefore argue that the **P** and **9 (22/*i*Pr$_2$)** oxidations have significantly different reasons for the large ΔE_p values observed; the peaks for **P** are separated principally because of very different electron-transfer kinetics for the ee and ae forms, while those of **9** are separated principally because of electron-transfer thermodynamics differences caused by gearing of the isopropyl groups, although use of the small k_s electrode platinum is necessary to observe large peak separations at 200 mV/s scan rates. AM1 calculations prove to be surprisingly useful for the estimation of λ'_{in} values of *N,N'*-cyclic tetraalkylhydrazines, including the experimental fact that ΔH_r(cat) is rather similar for even significantly twisted $\theta \simeq 120°$ *trans* hydrazines and θ near 180° *anti* ones, while it is significantly larger for *gauche* hydrazines, $\theta \simeq 60°$. AM1 calculations fail badly in other cases, such as **15**, and their use clearly requires suitable caution.

Experimental Section

2-*tert*-Butyl-3-neopentyl-2,3-diazabicyclo[2.2.2]octane (6). A vigorously stirred suspension of $\mathbf{3}^{+}BF_4^{-}$ [12] (1.5 g, 5.9 mmol) in dry THF (30 mL) contained in a 100-mL Schlenk flask at 0 °C under N_2 was treated dropwise with a neopentyllithium solution[39] (40 mL, 0.35 M, 14 mmol). The resulting mixture was stirred at 0 °C for 4 h, and after the solution had warmed to room temperature, the reaction was quenched with water and the aqueous layer was extracted with ether. The organic layers were dried with magnesium sulfate, and the residue, after solvent removal, was Kugelrohr distilled (0.6 mmHg, 163 °C bath temperature) to give 0.81 g (57.5%) of **6** as a light yellow oil. ^{1}H NMR ($CDCl_3$, 500 MHz): δ 3.08 (s, 1H), 2.95 (s, 1H), 2.88 and 2.42 (AB quartet, J = 13.5 Hz, 2H), 2.23 (tq, J = 13.2, 2.2 Hz, 1H), 1.96 (qt, J = 10.4 Hz, 1H), 1.78 (m, 2H), 1.66 (tdd, J = 11.2, 4.2, 1.1 Hz, 1H), 1.54 (tdd, J = 11.4, 3.8, 1.5 Hz, 1H), 1.32 (td, J = 12.2, 7.8 Hz, 1H), 1.20 (m, 1H), 1.15 (s, 9H), 0.95 (s, 9H). ^{13}C NMR ($CDCl_3$, 125 MHz): δ 70.0 (NCH_2), 57.7 (C_q), 48.6 (CH), 46.1 (CH), 32.0 (C_q), 29.8 (CH_3(tBu)), 29.6 (CH_2), 29.1 (CH_3(tBu)), 27.0 (CH_2), 21.5 (CH_2), 18.1 (CH_2). Empirical formula $C_{15}H_{30}N_2$ established by high-resolution MS.

Reaction of 6 with $NOPF_6$. A solution of $NOPF_6$ (73.9 mg, 0.42 mmol) in deaerated CH_3CN (1 mL) was added dropwise, via cannula, to a stirred solution of **6** (104.1 mg, 0.44 mmol)[12] in deaerated CH_3CN (7 mL) at 0 °C under Ar. Dry ether (250 mL) was added via cannula, which precipitated a light yellow solid. Filtration gave 93.9 mg of residue which was crystallized from CH_2Cl_2/ether at –20 °C to give a mixture concluded by integration of the bridgehead protons to consist principally of a ~6:1 ratio of aminoimmonium salt $\mathbf{10}^{+}PF_6^{-}$:neopentyl diazenium salt $\mathbf{11}^{+}PF_6^{-}$, which was not separated. **10**. ^{1}H NMR (CD_3CN, 500 MHz): δ 7.48 (s, 1H), 4.82 (br, 1H), 4.03 (br, 1H), 1.82–2.00 (m, 8H), 1.43 (s, 9H), 1.45 (s, 9H). ^{13}C NMR (CD_3CN, 500 MHz): δ 163.09 (CH), 63.87 (C_q), 63.87 (CH), 60.24 (CH), 35.79 (C_q), 29.46 (CH_3), 29.08 (CH_3), 25.57 (CH_2), 24.45 (CH_2). IR: 2973 cm^{-1}. **11**. ^{1}H NMR (CD_3CN, 500 MHz): δ 5.88 (br, 1H), 5.27 (br, 1H), 2.13 (~s, 2H), 1.10 (s, 9H) [CH_2 signals are complex and were not clearly identified]. ^{13}C NMR (CD_3CN, 500 MHz): δ 80.67 (CH_2), 71.62 (CH), 69.75 (CH), 27.61 (CH_3), 26.72 (CH_2), 23.17 (CH_2) [C_q was not located].

2-*tert*-Butyl-3-isopropyl-2,3-diazabicyclo[2.2.2]octane (7). Isopropylmagnesium chloride in THF (2 M, 4 mL, 8 mmol) was added dropwise to a stirring suspension of $\mathbf{2}^{+}BF_4^{-}$ (1.06 g, 4.2 mmol) in dry THF (20 mL) at room temperature, and after the solution was stirred overnight, the reaction was quenched with water (100 mL). After extraction with ether (3 × 50 mL), drying over magnesium sulfate, and concentration, Kugelrohr distillation gave an oil contaminated with a white solid. Filtration of a pentane solution through glass wool removed the solid, and solvent removal gave 458 mg (52%) of **7** as a colorless oil. ^{1}H NMR ($CDCl_3$, 500 MHz): δ 3.16 (sep, J = 6.9 Hz, 1H), 3.12 (br s, 1H), 2.99 (br s, 1H), 1.87 (m, 4H), 1.57 (m, 2H), 1.27 (m, 2H), 1.15 (d, J = 6.7 Hz, 3H), 1.06 (d, J = 7.0 Hz, 3H). ^{13}C NMR ($CDCl_3$, 500 MHz): δ 57.60, 55.17, 46.54, 46.35, 29.70 (CH_3(tBu)), 29.48 (CH_2), 28.57 (CH_2), 22.77 (CH_2), 22.60 (CH_2), 20.99 (CH_3(iPr)), 20.37 (CH_3(iPr)). ^{13}C NMR (CD_2Cl_2/$CFCl_3$, 500 MHz, referred to CD_2Cl_2 at 55.80 at 160 K; (type)[T_{max}, K; ν(^{1}/$_2$max), Hz]): δ(160 K) 57.66 (C_q)[180, 33.5], 55.55 (CH(iPr))[180, 34.7], 45.86 (NCH)[170, 13.6], 44.32 (NCH)[190, ~80], 29.16 (Me(tBu))[170, 15.5], 28.79 (CH_2)[170, 12.4], 28.22 (CH_2)[180, 33.2], 23.48 (CH_2)[190, ~80], 22.21 (CH_2)[180, 35.4], 20.92 (Me(iPr))[170, 13.9], 18.83 (Me(iPr))[190, ~80]. Empirical formula $C_{13}H_{26}N_2$ established by high-resolution MS.

2-*tert*-Butyl-3-isopropyl-2,3-diazabicyclo[2.2.2]octane Radical Cation Hexafluorophosphate ($\mathbf{7}^{\cdot+}$ PF_6^{-}). A solution of $NOPF_6$ (142.2 mg, 0.81 mmol) in deaerated CH_3CN (1 mL) was added dropwise to a stirred solution of **7** (167.8 mg, 0.80 mmol) in deaerated CH_3CN (11 mL) at –35 °C under Ar. After being stirred at –35 °C for 10 min, the golden yellow (or greenish) solution was treated with dry, ice-cold ether (200 mL), causing precipitation of a solid, and the solvent was removed via cannula. The solid was washed with 2 × 100 mL portions of ether and dried under N_2 to give 222.2 mg (78.5%) of $\mathbf{7}^{\cdot+}PF_6^{-}$, mp 178–9 °C dec. ^{1}H NMR (CD_3CN, 300 K): the NMR spectrum of 23.0 mg of $\mathbf{7}^{\cdot+}PF_6^{-}$ in 0.5 of mL deaerated CD_3CN was recorded at 500 MHz, with spectrometer settings SW = 166666.667 Hz, RD = 1.0, and NS ≃ 1200, and the spectrum was recorded after adding in succession 10-, 10-, 10-,

(39) Chang, B.-H.; Tung, H.-S.; Brubaker, C. H. *Inorg. Chem. Acta* **1981**, *51*, 143.

10-, 20-, and 20-μL aliquots of di-*tert*-butylnitroxide (5.96 M). The δ_{obs} values were plotted against total radical concentration. Table II shows the linearly extrapolated values to zero radical concentration as $\delta^{\cdot+}_0$. All other radical NMR spectra were obtained using the same technique.[17] Analysis was carried out on the NO_3^- salt, prepared using $AgNO_3$ oxidation, mp 124–5 °C dec. Anal. Calcd for $C_{13}H_{26}N_3O_3$: C, 57.33; H, 9.62; N, 15.43. Found: C, 57.50; H, 9.78; N, 15.54.

2,3-Diisopropyl-2,3-diazabicyclo[2.2.2]octane (9). A solution of isopropylmagnesium chloride in THF (2 M, 13.5 mL, 2.7 mmol) was added dropwise to a stirring suspension of 8^+I^- (3.02 G, 10.8 mmol)[12] in dry THF (20 mL) at room temperature, and after the solution was stirred overnight, the reaction was quenched with water (100 mL). After extraction with ether (3 × 50 mL), drying over magnesium sulfate, and concentration, Kugelrohr distillation gave **7** as a colorless oil, 1.55 g, 73.2%. ^1H NMR ($CDCl_3$, 500 MHz): δ 3.10 (br s, 2H), 2.87 (sept, J = 6.3 Hz, 2H), 1.97 (m, 2H), 1.77 (m, 2H), 1.67 (m, 2H), 1.26 (m, 2H), 1.07 (d, J = 6.5 Hz, 6H), 0.99 (d, J = 6.1 Hz, 6H). ^{13}C NMR ($CDCl_3$, 125 MHz): δ 54.02, 46.97, 27.79 (CH_2), 22.58 (CH_3), 21.93 (CH_3), 18.30 (CH_2). Empirical formula $C_{12}H_{24}N_2$ established by high-resolution MS.

2,3-Diisopropyl-2,3-diazabicyclo[2.2.2]octane Radical Cation Hexafluorophosphate ($9^+PF_6^-$). A sample of **9** (243.0 mg, 1.24 mmol) was treated with $NOPF_6$ (217.7 mg, 1.24 mmol) under exactly the same conditions as for the preparation of 7^+ above, giving 331.8 g (78.5%) of $9^+PF_6^-$ as a white solid, mp 200–1 °C dec. Analysis was attempted on the NO_3^- salt, prepared using $AgNO_3$ oxidation, mp 166–7 °C dec. Anal. Calcd for $C_{12}H_{24}N_3O_3$: C, 55.79; H, 9.36; N, 16.26. Found: C, 54.78; H, 9.24; N, 16.25 (C is unacceptably low).

Cyclic Voltammetry. An EG&E PAR Model 273 instrument interfaced to an IBM-XT was employed. Tetrabutylammonium perchlorate was recrystallized from hot 1:1 ethanol:water.

Acknowledgment. We thank for partial financial support of this work the National Institutes of Health under grant GM-29541 (SFN), the National Science Foundation under grants CHE-9100281 (DHE) and CHE-9105485 (SFN), and the Deutsche Forschungsgemeinschaft (FAN). Major instrument programs of both NSF and NIH supported the instrumentation used.

Supplementary Material Available: Figures showing the comparison of calculated and experimental cv curves under the same conditions as in Figure 3 at scan rates of 1.0, 0.5, 0.1, 0.05, and 0.02 V/s (6 pages). Ordering information appears on any current masthead page.